2017 International Conference on
Unmanned Aircraft Systems (ICUAS)
June 13-16, 2017, Miami, FL, USA

Development and Testing of the Intercept Primitives for Planar UAV Engagement

Satadal Ghosh* , Duane T. Davis** , Timothy H. Chung*** , and Oleg A. Yakimenko****

Abstract— **With the advance in technologies and applications involving unmanned aerial systems cooperation among the autonomous agents within such an unmanned system as well as preparedness for responding to adversarial threat to such a system has become of pivotal importance. A multi-phase operational scenario of such cooperative and adversarial engagement, motivated by manned aerial engagement scenarios, is presented in this paper. A Proportional navigation-based integrated guidance methodology is proposed and investigated as a candidate strategy for intercept primitives in such realistic multi-phase UAV engagements. Numerical examples are presented to demonstrate the performance of the proposed guidance strategy for an UAV in such an engagement. Finally, implementation of these guidance laws in a waypoint-based manner, well suited for use in modern-day autopilots of UAVs, is demonstrated in software-in-the-loop simulations, further accelerating future live-fly capabilities for autonomous aerial engagements.**

I. Introduction

Because of the advantages of low cost, quite less human risk, and ease in portability, aerial robots such as unmanned aerial vehicles (UAV) have found ever-increasing applications in last few years. The applications of UAVs envisaged so far range from scientific application like scientific data gathering to civilian applications like pollutant monitoring, search for and rescue of survivors of accidents or disasters, forest fire surveillance, wildlife management, geological surveys to military applications like security, surveillance and reconnaissance, patrolling border, bomb detection, unmanned intelligence gathering operations, and so on. Advances in communication, actuation, and battery technology have further added to the capabilities of the UAVs [1].

Coupled with these many advances is an increasing interest and need for benchmarking and performance metrics for robotics [2]. Among the considerations for integrating test and evaluation methodologies in the development of autonomous behaviors is the definition of *systems-level* operational scenarios. Leveraging such holistic use cases as benchmarks enable constructive and communal advancement of technologies, while ensuring that there is consistency in the desired performance outcomes and that they are tied to mission-oriented measures. To this end, this paper develops an intercept primitive in the form of a multi-phase operational scenario for a planar UAV-UAV engagement in an unmanned aerial system (UAS). Motivated by manned aerial engagement scenarios, this notion further provides a demonstrable test framework for UAV engagements, and could be helpful for assessing test algorithms for such engagements.

Apart from different decision making steps in different phases, two relevant components, namely path-following with a feature of angular control, and guidance for pursuit, are of prime interest to devise an integrated strategy for this multi-phase operational scenario. There is a wide body of existing literature on both path-following and guidance for unmanned vehicles. In many of the existing literature on path-following, traditional control methodologies have been explored. For example, a gain-scheduling control was discussed on linearized form of nonlinear equations of motion in [3] to track reference trajectories defined in an inertial reference frame, while [4] studied the path-following problem using a Lyapunov based piecewise-affine control law. On the other hand, some of the related literature has studied this problem from the view-point of guidance also. [5] presented a concept of guidance-based path following using a parameterized geometry of the trajectory to be tracked. [6], [7] presented a nonlinear guidance logic which approximates a proportional-derivative controller of cross-track error when close to the trajectory to track with an additional element of anticipatory control enabling tight tracking when following curved paths. This guidance logic is similar to proportional navigation (PN) law against a virtual stationary target that moves every time-instant. [8] obtained differential geometric expressions for orbits that allow an aircraft to keep flight paths that result in constant line of sight with respect to the aircraft body-fixed frame. [9] presented a synthetic-waypoint guidance algorithm which attempts to emulate pure pursuit (PP) guidance law and showed that its performance depends on a guidance parameter - the desired time horizon for the vehicle to initiate a response to flight path changes. For tracking of circular paths by UAVs [10] analyzed a guidance law which has also a similarity with PN guidance law against a stationary virtual target that is moved with time. The trajectory shaping guidance in [11] has been investigated in [12] for virtual target following on a planar path and its advantage over PP based method [9] has been shown.

* Satadal Ghosh is with the Department of Systems Engineering at Naval Postgraduate School, Monterey CA. This research was performed while Satadal Ghosh held an NRC Research Associateship award at the Naval Postgraduate School. sghosh@nps.edu

** Duane T. Davis is with the Cyber Academic Group at Naval Postgraduate School, Monterey CA. dtdavi1@nps.edu

*** Timothy H. Chung is with the Tactical Technology Office at DARPA, Arlington VA. timothy.chung@darpa.mil

**** Oleg A. Yakimenko is with the Department of Systems Engineering at Naval Postgraduate School, Monterey CA. oayakime@nps.edu

978-1-5090-4494-8/17/$31.00 ©2017 IEEE

The other relevant component of the present work, that is Guidance, has been studied mostly for interceptor-target engagements. Broadly guidance laws can be classified as classical or empirical guidance laws, and modern guidance laws [13], [14]. Pursuit (pure pursuit and deviated pure pursuit) guidance and Constant bearing guidance fall under the category of classical and conceptual guidance philosophies. One of the implementable classical guidance laws is the Line-of-sight (LOS) guidance, in which the interceptor is fired in the direction of the target and made to remain on the LOS joining the launch station and the target. But, the most important guidance law of all the classical ones is the proportional navigation (PN) guidance law, which emulates the principle of constant bearing course in the most logical way, in which to ensure zero LOS rate the interceptor's turn rate is made proportional to the LOS rate. [15], [16] presented the seminal work on the capturability analysis of pure PN (PPN) guidance law, while [17] presented an approximate closed form solution of the PPN guidance. [18] presented analysis of true PN (TPN) guidance against a maneuvering target. On the other hand, modern guidance laws are developed based on optimal control [19], [11], sliding mode control [20], differential geometry [21], and so on. Interestingly, in a linearized engagement geometry against a moving but non-maneuvering target, TPN was shown to be optimal in [22]. And, for aerodynamically driven vehicles like fixed-wing UAVs PPN is more suited option than TPN. In this work, therefore, variants/augmentation of PPN has been considered to develop the guidance strategy for the proposed intercept primitive problem.

The main contribution of this paper includes development of a holistic notion of an intercept primitive for a planar UAV-UAV engagement in the form of a multi-phase operational scenario and devising an integrated PPN-based guidance as a candidate strategy for such an engagement. Numerical simulation results demonstrate the problem and the mission-oriented effectiveness of the developed integrated PPN-based guidance strategy for this problem. Implementation of these guidance laws in a waypoint navigation-based manner, suitable for most modern-day autopilots, including those used in NPS swarm UAV live-fly testbed [23], [24], is demonstrated by software-in-the-loop integrated simulations.

The paper is organized with the formulation of the two-UAV engagement primitive problem in Section II, with a proposed solution approach based on proportional navigation methods and simulation results highlighted in Sections III and IV, respectively. Further implementation in integrated flight software, as demonstrated in software-in-the-loop simulation for an operational live-fly testbed, is provided in Section V. Concluding remarks and numerous avenues for future work are detailed in Section VI.

II. An UAV-UAV Engagement Problem Formulation

As highlighted in the previous section, study of interactions between aerial agents (e.g., UAVs, manned aircraft), whether cooperative or non-cooperative, provides the motivation for the multi-phase operational scenario considered in this paper. Consider two fixed-wing UAVs, which obey nonholonomic kinematic equations of motion, each with respective flight characteristics of speed and maneuverability. The two UAVs are initially positioned in the two-dimensional plane at some separation or standoff distance and with arbitrary initial headings. Let the Blue UAV (a.k.a. the pursuer) have fixed speed v_P and maximum turn rate $\dot{\alpha}_P^{\max}$, and let the Red UAV (a.k.a. the target) have fixed speed v_T and maximum turn rate $\dot{\alpha}_T^{\max}$. The relative bearing of the Red UAV from the perspective of the Blue UAV lies along the Line-of-Sight (LOS) between the two aircrafts. The UAVs are capable of estimating the each other's position and speed, either using onboard sensors for example, visual detection and tracking, transponder signals like automatic dependent surveillance-broadcast (ADS-B), or by being provided such data through ground radar systems or telemetry feeds. Generally speaking, the operational scenario dictates that the Red UAV transits towards the Blue UAV's area of operations, and the Blue UAV must maneuver appropriately to respond to the Red UAV's approach in some manner during the two phases of the UAV-UAV engagement, illustrated in Figure 1 and described next in greater detail.

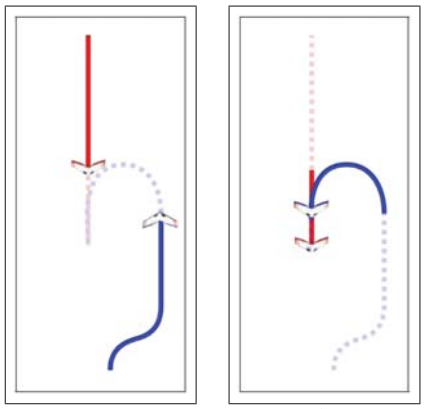

Fig. 1. Schematic of a UAV-UAV engagement operational scenario. As Blue and Red UAVs approach one another, (a) the Blue UAV maneuvers to align itself on a course parallel to the Red UAV's path. (b) At the appropriate relative position, the Blue UAV turns towards the Red UAV to intercept (adversarial target case) or rendezvous (cooperative target case).

A. Phase I: Maneuver to Track

The first phase, as shown in Figure 1(a), represents the initial maneuver by the Blue UAV towards a course that is parallel but in opposite direction to that of the Red UAV, and offset by a pre-specified lateral separation distance. Such a maneuver may be relevant to avoid mid-air collisions, e.g., in congested airspaces, or to improve sensing vantage points for improved tracking and estimation, or to avoid the target's effective sensing zone.

Solutions to this subproblem, for a given desired lateral separation distance between the parallel courses, should: (a) provide a decision rule for selecting which side (for example,

left or right in the planar engagement case) of the incoming Red UAV's course to follow, and also (b) provide a guidance strategy (or algorithm or policy) to efficiently maneuver the Blue UAV to align with the selected parallel course.

B. Phase II: Maneuver to Intercept (Rendezvous)

Figure 1(b) illustrates the second phase, in which the Blue UAV keeps on tracking the Red UAV while moving along the predefined parallel course, obtained from Phase I. Once the Red UAV comes closer to the Blue UAV by a pre-specified threshold distance, it has to depart from the parallel course and maneuver to intercept or contain (in case of adversarial target) or rendezvous (in case of cooperative target) with the Red UAV. These types of maneuvers are often found in formation or cooperative control contexts, such as flocking, mid-air refueling operations, docking and aerial delivery of products, etc., or in following/chasing/containing a target.

This subproblem first calls for a decision making rule to determine when to initiate the maneuver of the Blue UAV to the target. Then, a suitable guidance strategy is needed to satisfy relevant engagement parameters of this subproblem that include the desired intercept angle (a.k.a. approach angle) with respect to the course of Red UAV (e.g., an angle, π, denotes the Blue UAV's head-on approach to the Red UAV) and the desired final separation distance from the Red UAV (e.g., zero distance implies a collision/interception). The desired final angle and distance are relevant to ensure that the Red UAV lies within the shooting zone of the Blue UAV, and hence is contained by the pursuer at the final time-instant.

III. Integrated Proportional Navigation-based Approach for UAV-UAV Engagement

A. Proportional Navigation for UAV Engagement

The basic principle of proportional navigation guidance [13], [14] is to control the autonomous agent's heading turn rate, $\dot{\alpha}$, such that the line-of-sight (LOS) turn rate (typically denoted $\dot{\theta}$) is driven to zero, which is typically termed as formation of 'collision course' with the target. Coupled with the agent's fixed forward speed, the agent achieves a positive closing rate (i.e., diminishing range to target), thereby enabling successful arrival on target. As its name implies, for proportional navigation, the generated guidance command is proportional to the LOS turn rate. There are several variants of proportional navigation studied in the literature (see [13], [14] for seminal and survey works), which are distinguished by the direction of the application of guidance commands and the proportionality constants. Since pure proportional navigation (PPN) is most suitable for aerodynamically driven vehicles (such as the fixed-wing UAVs considered), in this work we specifically consider a family of PPN-based guidance strategies, where the proportionality constant is given as a product of some navigation gain, N, and the pursuer's speed. Throughout all these phases of this problem, the Blue UAV uses one or more augmented variants of PPN to guide its flight, which simplifies the interfaces necessary for physical field implementation as well as provides a baseline for further research and development, including different methods to address different phases.

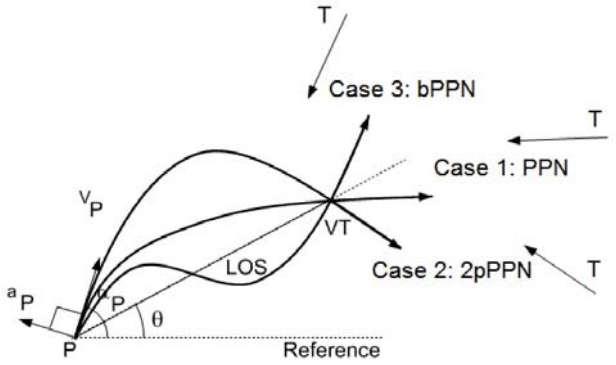

Fig. 2. Engagement geometry of Phase I and different headings of Blue UAV at virtual target

B. Strategy for Phase I: Manuever to Track

1) Background: In the proposed approach, as soon as the Blue UAV senses that the red UAV is within a prescribed standoff distance R_1 with respect to the Blue UAV, it computes a stationary *virtual target* (VT) point, with desired lateral offset distance from the target's course, and a desired heading angle at VT, so as to align with this parallel course. As seen in basic engagement geometry for this phase in Fig. 2, depending on the initial conditions of the scenario (e.g., relative headings of both Blue and Red UAVs), there are three possible cases of different relative headings that call for different augmented forms of PPN to reach the virtual target point in a heading angle-constrained manner.

2) Some results: For this phase, consider a planar pursuit between a virtual stationary target VT and a PPN guided pursuer P with constant speed V_P as shown in Fig. 2. The kinematic equations of motion are given in terms of relative velocity along and across the range (V_R and V_θ, respectively) as,

$$V_R = \dot{R} = -V_P \cos(\alpha_P - \theta) \tag{1}$$

$$V_\theta = R\dot{\theta} = -V_P \sin(\alpha_P - \theta) \tag{2}$$

$$\dot{\alpha}_P = a_P / V_P = N\dot{\theta} \tag{3}$$

where, α_P is the pursuer's heading angle and θ is the LOS angle between the pursuer and the VT. The pursuer's lateral acceleration is given by $a_P = NV_P\dot{\theta}$, and N is the navigation gain. In Section III-B, θ denotes the LOS angle between the pursuer and VT. Without loss of generality (WLOG) the inertial reference frame can be considered such that $\alpha_{P_0} > \theta_0$. Then, by standard PPN guidance, the heading angle of the Blue UAV at VT at the end of Phase I $\alpha_{P_{f_1}} \in [2\theta_0 - \alpha_{P_0}, \theta_0)$ for $N \geq 2$, with $\alpha_{P_{f_1}} = \theta_0$ attained by $N \to \infty$. However, by using a two-phase PPN (2pPPN) guidance strategy discussed in [25], the set of achievable impact angles could be further extended to a set $\alpha_{P_{f_1}} \in [-\pi + \theta_0, \theta_0)$. The achievable heading angles by using standard PPN or 2pPPN are represented in Fig. 2.

However, note that in this problem the operational scenario could present a situation (case 3 in the figure) where the desired heading of the Blue UAV could be outside the aforementioned achievable set. In fact, Case 3 could well be a quite frequently encountered scenario. Now, the possibility of achieving a further set of impact angle at the virtual target by bias-based augmentation of PPN would be discussed below.

It can be easily shown that for standard PPN or two-phase PPN in [25], the LOS rate does not change its sign. However, the situation 3 shown in Fig. 2, which appears frequently in the problem under consideration, clearly necessitates a change in the sign of LOS rate to achieve the desired heading of the Blue UAV at the VT. Although biased PN guidance has been discussed in the guidance literature [26], the use of pulsed biases for the purpose of reversal of LOS rotation has been described in [27] to achieve an expanded set of impact angles against higher speed targets. In a similar way, the following result can be proved.

Lemma 1: Addition of a bias profile $B\,\mathrm{sgn}(\dot{\theta}_0)$, nonzero for a certain time interval, to the PPN guidance command with $N \geq 2$ can achieve the reversal of sign of $\dot{\theta}$.

Let the combination of bias as in Lemma 1 over the underlying PPN guidance be termed as bPPN.

Theorem 1: Using standard PPN or 2pPPN or bPPN followed by PPN or 2pPPN, an expanded heading angle set at the virtual target can be achieved.

Proof: WLOG consider $\alpha_{P_0} > \theta_0$. By using standard PPN or 2pPPN, the achievable heading angle set is $\alpha_{P_{f_1}} \in [-\pi + \theta_0, \theta_0)$ as discussed earlier.

Now, consider the bias profile in case of bPPN (as in Lemma 1) to be applied to the pursuer's guidance command from time $t_1 \geq t_0$. This first leads to monotonic decrease of θ_P and hence $|V_\theta|$ to zero first, which signify the reversal of the direction of rotation of LOS. Use of bPPN for further some time ensures further decrease of α_P and increase of θ, which implies that an LOS angle θ_2 is achieved such that $\alpha_{P_{f_1}} \in [\theta_2, \theta_2 + \pi)$, which could be attained by using PPN or 2pPPN from that time-point onward.

Thus, the expanded set of achievable heading of the pursuer at the virtual target could be given as $\alpha_{P_{f_1}} \in [-\pi + \theta_0, \theta_0) \cup [\theta_2, \theta_2 + \pi)$, which proves the theorem. ■

Details of these results could be found in [28].

3) Algorithm (P1): Based on the above discussion, the following algorithm for Phase I is described.

1) Initialize with Red UAV position
2) Estimate Red UAV course α_T
3) Determine location of virtual point (VT) to satisfy offset distance requirement
4) Calculate the desired heading angle of the Blue UAV at VT at the end of Phase I $\alpha_{P_{f_1}} = \alpha_T + \pi$.
5) Check value of $\alpha_{P_{f_1}}$
   a) If $\alpha_{P_{f_1}} \in [2\theta_0 - \alpha_{P_0}, \theta_0)$, then use standard PPN with navigation gain, $N = (\alpha_{P_{f_1}} - \alpha_{P_0})/(\alpha_{P_{f_1}} - \theta_0)$.
   b) If $\alpha_{P_{f_1}} \in [-\pi + \theta_0, 2\theta_0 - \alpha_{P_0})$, then use 2pPPN as in [25].
   c) Else use bPPN as in Lemma 1 with $N = 2$ and bias $B\,\mathrm{sgn}(\dot{\theta}_0)$ where B is finite positive, until some time t_2 at which $\theta = \theta_2$ and $\alpha_P = \alpha_{P_2}$, such that $\alpha_{P_{f_1}}$ falls within the interval $[\theta_2, \theta_2 + \pi)$. At time t_2, go to Step 5d.
   d) If $\alpha_{P_{f_1}} \in [\theta_2, 2\theta_2 - \alpha_{P_2}]$, use standard PPN with $N = (\alpha_{P_{f_1}} - \alpha_{P_2})/(\alpha_{P_{f_1}} - \theta_2)$.
   e) If $\alpha_{P_{f_1}} \in (2\theta_2 - \alpha_{P_2}, \pi + \theta_2)$, use 2pPPN as in [25].

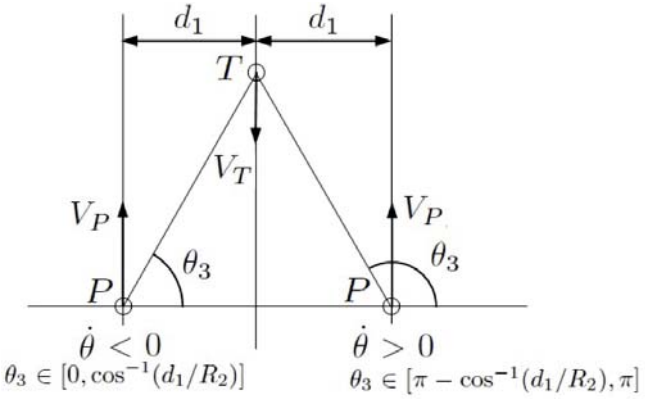

Fig. 3. Engagement geometry at the initial part of Phase II

C. Strategy for Phase II: Maneuver to Intercept (Rendezvous)

1) Background: In this phase, the Blue UAV tracks the motion of the Red UAV, and as the range between the two UAVs becomes less than another threshold standoff distance R_2, the former starts approximating the required control effort to maneuver by using PPN towards a capture or shoot-to-kill point at a particular heading (dependent on the angular range of pursuer's weapon) with respect to the latter. The Blue UAV must also determine a suitable time-instant of initiation of the maneuver towards the capture or shoot-to-kill point.

2) Approximation of overall control effort: Consider a planar pursuit between a target T and a pursuer P, as shown in Fig. 3, where V_T is the target's constant speed, and a_T is its lateral acceleration. For the present phase, the target (red UAV) is nonmaneuvering, that is $a_T = 0$. In this phase, θ denotes the LOS angle between the Blue and Red UAVs. The kinematic equations of motion of the engagement are given as,

$$V_R = \dot{R} = V_T \cos(\alpha_T - \theta) - V_P \cos(\alpha_P - \theta) \quad (4)$$

$$V_\theta = R\dot{\theta} = V_T \sin(\alpha_T - \theta) - V_P \sin(\alpha_P - \theta) \quad (5)$$

$$\dot{\alpha}_P = a_P/V_P = N\dot{\theta}; \quad \dot{\alpha}_T = a_T/V_T = 0 \quad (6)$$

where, the pursuer's lateral acceleration is given by $a_P = NV_P\dot{\theta}$, and N is the navigation gain in this phase given as,

$$N = (\alpha_{P_{f_2}} - \alpha_{P_1})/(\theta_{f_2} - \theta_3) > 0 \quad (7)$$

where, $\alpha_{P_{f_2}}$ is the desired heading of the pursuer at the shoot-to-kill point, and θ_{f_2} is given as $\theta_{f_2} = \tan^{-1}[(V_T \sin\alpha_T - V_P \sin\alpha_{P_{f_2}})/(V_T \cos\alpha_T - V_P \cos\alpha_{P_{f_2}})]$ with $\theta_{f_2} > \theta_3$ ($< \theta_3$) for positive (negative) LOS rate. From (6), the evolution of $\theta_P = \alpha_P - \theta$ and $\theta_T \triangleq \alpha_T - \theta$ (for $a_T = 0$) can be given as,

$$\dot{\theta}_P = (N-1)\dot{\theta};\ \ \dot{\theta}_T = -\dot{\theta} \tag{8}$$

And, suppose that the maneuver of the pursuer begins at time $t = t_3$, $\theta = \theta_3$, and the shoot-to-kill point is reached at time t_{f_2}, $\theta = \theta_{f_2}$. Then, from (4) and (5), range R and overall control square integral (E) are given as,

$$R(\theta) = R(\theta_3)\exp[\int_{\theta_3}^{\theta}(V_R(\psi)/V_\theta(\psi))d\psi]; \tag{9}$$

$$E = (N(\theta_3)V_P)^2 \int_{\theta_3}^{\theta_{f_2}} V_\theta/R d\theta \tag{10}$$

PPN guidance law strives to reach collision course $(\theta = \theta_{f_2})$ at which LOS rate is zero, and once the collision course is achieved, the guidance command becomes zero. This feature allows us to express E in terms of the transformed independent variable θ instead of time t. This also helps in developing a numerical integration algorithm for approximating E, which is simple, but fast and efficient. Specifically, a numerical iterative approximation algorithm of E similar to the numerical iterative algorithm presented in [29] for approximating time-to-go is considered for any time-instant t after the range between the blue and red UAVs becomes less than the prescribed safety standoff value R_2.

3) Decision on maneuver initiation: Note from (10) that the overall control effort E for the maneuver in this phase is clearly a function of the initiation time-point of maneuver or equivalently the LOS angle θ_3 at the time of initiation of Blue UAV's maneuver to the Red UAV. Also, for $\dot{\theta} > 0$ (< 0), that is for $\theta_{f_2} > \theta_3$ $(< \theta_3)$, $\theta_3 \in [\pi - \cos^{-1}(d_1/R_2), \pi]$ $([0, \cos^{-1}(d_1/R_2)])$ as shown in Fig.3. It can be shown that the overall control square integral in the maneuvering part of this phase, that is E, is convex in θ_3 over its domain for a given combination of d_1, R_2 and ν. A typical E Vs. θ_3 is shown in Fig. 4, which clearly shows how closely the numerical iterative approximation algorithm of E discussed in Section III-C.2 matches with the actual values for different maneuver-initiation points. Hence, a greedy approach with an additional history-based rectification feature in decision making about the initiation of the maneuver of the Blue UAV is justified based on the minimal value of estimated E. Based on these, the algorithm of second phase is discussed in next section.

4) Algorithm: Let the profile of LOS rate corresponding to the parallel paths of blue and red UAVs followed from the end of first phase be called as $\dot{\theta}_{nom}$.

1) Maintain the same heading α_P as obtained from the first phase. Track the motion of the red UAV. If it maneuvers away $(|\dot{\theta}| < |\dot{\theta}_{nom}|)$, or remains in its straight path $(|\dot{\theta}| = |\dot{\theta}_{nom}|)$, maintain same heading and keep tracking it. If it maneuvers closer $(|\dot{\theta}| > |\dot{\theta}_{nom}|)$, then initiate first phase if $R \geq R_2$, and initiate maneuver towards the target if $R < R_2$. Otherwise, go to Step 2.
2) Compute the required gain N to maneuver using PPN to the capture or shoot-to-kill point with respect to the red UAV at the desired heading as given in (7). Estimate overall control energy square integral E using numerical iterative algorithm in Section III-C.2. Check if the present estimated E value is less than the estimated value of E at last time-instant. If yes, then maintain same heading. Else, start maneuver using PPN guidance command with navigation gain N.
3) Keep on maneuvering as mentioned in Step 2 until the capture or shoot-to-kill point with respect to the red UAV is reached at desired heading or the red UAV starts maneuvering, whichever happens earlier.

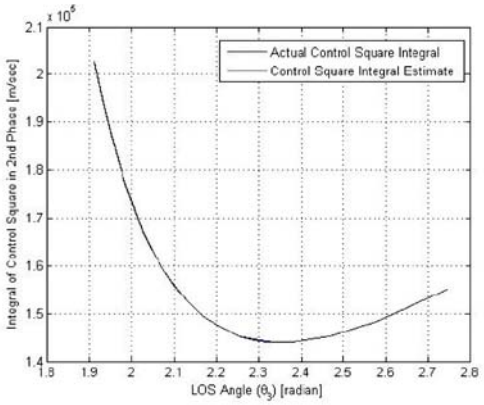

Fig. 4. Overall control square integral Vs. θ_3

Note that this phase ends the two-phase operational scenario, which is relevant for two major equivalent problems in an unmanned air system. One of them is rendezvous with the Red UAV (a cooperative case), while the other one is the neutralization of a passive threat problem. However, if the red UAV is indeed capable of weapons and starts maneuvering to evade or hit a reverse attack, this operational scenario could lead to an end-game phase of close combat. However, such a close combat scenario is kept out of the scope of this paper.

IV. Simulation Studies

In this section two major scenarios would be considered. The first scenario corresponds to the problem of product delivery to a desired stationary destination following a particular final orientation as shown in Section IV-A, while in the second scenario, shown in Section IV-B, the target or the red UAV is passive, that is it maintains straight path throughout. The simulation parameters are:

Initial range $R_0 = 1440$m, $V_P = 20$m/sec, $V_T = 12$m/sec (in case of moving red UAV in Section IV-B), $a_{P_{max}} = 4.8$m/sec^2. Threshold range for first phase initiation $R_1 = 1400$m; parameters for virtual target localization $d_1 = 200$m, $d_2 = 360$m, threshold range for starting of E estimation in second phase $R_2 = 400$m; shooting range $R_{sh} = 8$m,

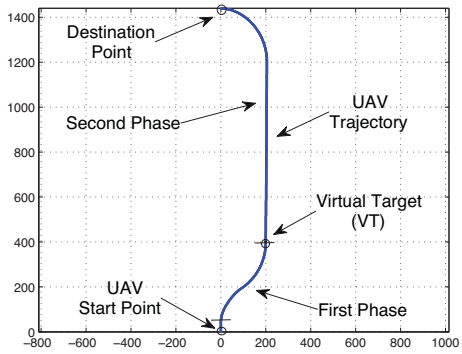

Fig. 5. UAV trajectory in mission for stationary destination

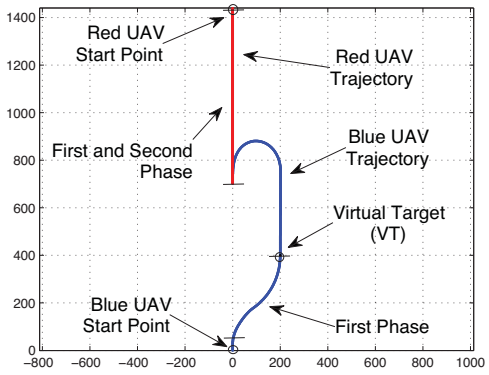

(a) Aligned Target

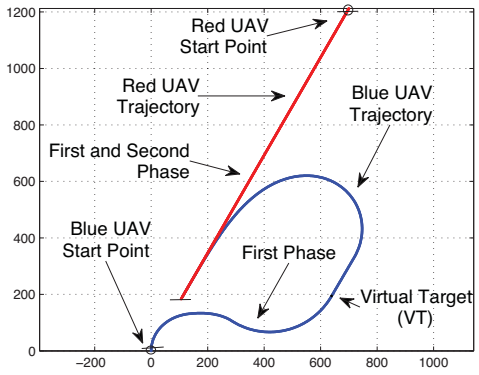

(b) Generic Target

Fig. 6. Trajectories against passive red UAV

shooting angle $\phi_{sh} = \cos^{-1}(0.8)$, for recursive steps for E estimation $\theta_{step} = 0.0025$. The simulations are run in 10Hz frequency of guidance commands.

A. Mission for stationary destination

For the mission of product delivery at stationary destination with desired final approach angle π, the UAV is required to reach the VT with a heading $(\alpha_{P_{f_1}})$ equal to its initial LOS angle $\pi/2$ with the destination for some operational requirement. The LOS angle with the VT at the beginning of first phase, $\theta_{VT_0} = 1.0637$. Since $(\alpha_{P_{f_1}})$ does not lie in the interval $[-\pi + 1.0637, 1.0637]$, the bPPN followed by PPN guidance, presented in Section III-B.3, is applied to the UAV. Note that since bPPN followed by PPN is a contribution of this paper, in simulation studies scenarios requiring this strategy have been investigated. As can be noticed from the trajectory of the UAV shown in Fig. 5, the UAV follows bPPN followed by PPN to reach VT with $\alpha_{P_{f_1}} = \pi/2$. In the second phase, it starts estimating control square integral E when the range falls below $R_2 = 400$m. Based on the algorithm, presented in Section III-C.4, it starts maneuvering towards the destination in the second phase using PPN with navigation gain $N = 1.2958$ when minimum E is obtained at range equal to 317.26m, and LOS angle $\theta_3 = 2.2746$. Finally, it reaches the destination at an angle $\alpha_{P_{f_2}} = \pi$.

B. Mission against passive Red UAV

A mission against a non-maneuvering passive red UAV is shown in Fig. 6. For aligned target, VT is located 200m ahead from the pursuer and 360m away from target's path, while for generic target, VT is selected arbitrarily at around 525m distance from the target's straight trajectory. Here, the requirement of the first phase is to reach the VT with a heading $(\alpha_{P_{f_1}}) = \alpha_{T_0} + \pi = \pi/2$ for aligned target in Fig. 6(a), and $\alpha_{P_{f_1}} = \alpha_{T_0} + \pi = \pi/3$ for a generic target in Fig. 6(b), followed by the final approach to the red UAV in a tail-chase mode. The LOS angle with the VT at the beginning of first phase, $\theta_{VT_0} = 1.0637$ and 0.303 for aligned and generic target, respectively. Since $(\alpha_{P_{f_1}})$ does not lie in the interval $[-\pi + \theta_{VT_0}, \theta_{VT_0}]$ in modulo 2π sense in either case, the bPPN followed by PPN guidance, presented in Section III-B.3, is applied to the Blue UAV for both the targets in Phase I to achieve desired $\alpha_{P_{f_1}}$ at VT. In Phase II, the Blue UAV starts estimating control square integral E when the range falls below $R_2 = 500$m with a requirement of $\alpha_{P_{f_2}} = \theta_{f_2}$ equal to $3\pi/2$ and $4\pi/3$ in case aligned and generic target, respectively, which is same as α_{T_0} modulo 2π. Following the algorithm in Section III-C.4, minimum E is sensed at range values 284.11m and 497.72m, respectively, and corresponding $\theta_3 = 2.3609$ and 2.211, respectively, and the Blue UAV starts maneuvering using PPN with $N = 1.3382$ and 1.5916, respectively, and reaches the non-maneuvering red UAV in a tail-chase mode with desired final angles.

V. Software-in-the-Loop Implementation

In order to facilitate rapid development and deployment for live-fly UAV field experiments, we actively employ software-in-the-loop (SITL) simulation capabilities that allow for testing with flight-ready software. As described in [23], use of SITL leverages a software emulation of the (Pixhawk/Ardupilot) autopilot and provides a realistic, physically-based flight dynamics response. Multiple instances of the SITL simulator can run simultaneously either on a single computer, on a cluster, or on networked com-

puters to facilitate experiments with more than 50 simulated UAVs. The system is also capable of interacting with live UAVs, making it possible to incorporate simulated UAVs into live-fly events [23].

Multi-UAV coordination and autonomy for the NPS (Naval Postgraduate School) system is implemented on a companion computer running Ubuntu 14.04 Linux and the Robot Operating System (ROS) [24]. The companion computer communicates with the Pixhawk autopilot over a serial connection that is simulated by the SITL implementation. The ability to run actual UAV software in a realistic simulated environment has been instrumental in supporting the agile development processes that have enabled an aggressive implementation and testing schedule [23].

Autonomous behaviors are implemented using a multi-process software architecture that relies on ROS services and message topics for inter-process communication and synchronization. Each behavior is implemented within this architecture as an independent ROS node as described in [24]. The autonomous engagement algorithms presented in this paper are implemented as behaviors in this architecture for testing in the SITL environment and ultimately in live-fly experiments.

Figs. 7(a)-(f) depict snapshots of an illustrative example of the proportional navigation-based approach described here as executed in the SITL virtual environment. This example showcases how the pursuing UAV (labeled "UAV102") transits and maneuvers to engage with the nonreactive target UAV ("UAV101", starting from west and moving east). For this simulation, realistic flight and operational parameters are used, i.e., flight speeds of UAVs, $V_P = 22.11$m/s, $V_T = 17.16$m/s; offset distances set to $d_1 = 200$m, $d_2 = 360$m; range thresholds set to $R_1 = 1400$m, $R_2 = 500$m. To implement the PPN based guidance commands a_P for the Blue UAV and the guidance commands $a_T = 0$ for the Red UAV (according to its strategies) in the SITL setup, the following relations are used for the generation of waypoints (x_{L_1}, y_{L_1}) for both blue and Red UAVs.

$$
\begin{aligned}
&L_1 = L_{1_{fixed}} = 150m; \\
&\eta_P = \sin^{-1}(a_P L_1/2V_P^2); \eta_T = \sin^{-1}(a_T L_1/2V_T^2) \\
&x_{L_{1_P}} = x_P + L_1 cos(\alpha_P + \eta_P); \\
&y_{L_{1_P}} = y_P + L_1 cos(\alpha_P + \eta_P) \qquad (11) \\
&x_{L_{1_T}} = x_T + L_1 cos(\alpha_T + \eta_T); \\
&y_{L_{1_T}} = y_T + L_1 cos(\alpha_T + \eta_T) \qquad (12)
\end{aligned}
$$

In SITL simulations, in order to smooth out perturbations and noises in the execution of the gradient based greedy approach in Step 2 of algorithm P2 of Phase II, the comparison of estimated value of E was done with respect to the minimum of mean and median of the estimated E values over last 10 time-instants instead of just the previous time-instant.

VI. Conclusion

A holistic intercept primitive problem for planar UAV-UAV engagement has been presented in this paper, which could be useful as a testbed to analyze the different UAV capabilities in varied multi-phase operational scenarios. Considering the optimality property of proportional navigation-based guidance laws, a strategy for this two-phase operational scenario has been proposed using several variations of proportional navigation. Besides several numerical examples, the proposed control solutions have also been implemented in a realistic UAV autopilot waypoint-navigation framework using software-in-the-loop simulations. This opens up great potential in the application of the traditional guidance laws, generally discussed in the context of interceptors, for path-following and waypoint-navigation problems of UAVs. Future work includes addition of an end-phase of close combat to this two-phase mission, and live-fly field experimentation of one-to-one and many-to-many UAV-UAV engagements for further development of several swarm engagement capabilities.

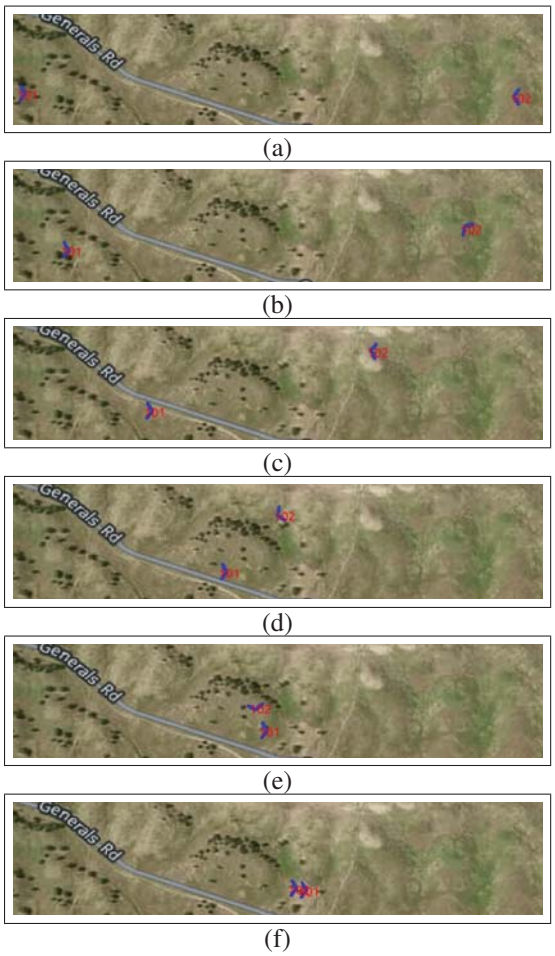

Fig. 7. Snapshots of an illustrative run of the software-in-the-loop (SITL) simulation environment of the UAV-UAV engagement benchmark problem. (a) The target UAV starts from the west and transits east; (b) the pursuer UAV maneuvers towards a virtual point, to (c) align on a parallel course; (d) the pursuer UAV turns into the target UAV, (e) achieving an intercept heading, and (f) resulting in a successful tail-chase engagement.

ACKNOWLEDGEMENT

The authors would like to thank the Consortium for Robotics and Unmanned Systems Education and Research at the Naval Postgraduate School for funding this research.

REFERENCES

[1] R. Beard, D. Kingston, M. Quigley, D. Snyder, R. Christiansen, W. Johnson, T. McLain, and M. Goodrich, "Autonomous vehicle technologies for small fixed wing UAVs," *AIAA Journal of Aerospace Computing, Information, and Communication*, vol. 2, no. 1, pp. 92–108, 2005.

[2] F. Bonsignorio, A. P. del Pobil, and E. Messina, "Fostering progress in performance evaluation and benchmarking of robotic and automation systems [tc spotlight]," *IEEE Robotics Automation Magazine*, vol. 21, no. 1, pp. 22–25, March 2014.

[3] I. Kaminer, A. Pascoal, E. Hallberg, and S. C., "Trajectory Tracking for Autonomous Vehicles: An Integrated Approach to Guidance and Control," *AIAA Journal of Guidance, Control, and Dynamics*, vol. 21, no. 1, pp. 29–38, Jan 1998.

[4] S. Shehab and L. Rodrigues, "Preliminary results on UAV path following using piecewise-affine control," in *Control Applications, 2005. CCA 2005. Proceedings of 2005 IEEE Conference on*, Aug 2005, pp. 358–363.

[5] M. Breivik and T. Fossen, "Principles of Guidance-Based Path Following in 2D and 3D," in *Decision and Control, 2005 and 2005 European Control Conference. CDC-ECC '05. 44th IEEE Conference on*, Dec 2005, pp. 627–634.

[6] S. Park, J. Deyst, and J. How, "A new nonlinear guidance logic for trajectory tracking," in *AIAA Guidance, Navigation and Control Conference*, Dec 2004, AIAA 2004-4900, pp. 627–634.

[7] ——, "Performance and lyapunov stability of a nonlinear path-following guidance method," *AIAA Journal of Guidance, Control, and Dynamics*, vol. 30, no. 6, pp. 1081–1089, Nov 2007.

[8] R. Rysdyk, "Unmanned Aerial Vehicle Path Following for Target Observation in Wind," *AIAA Journal of Guidance, Control, and Dynamics*, vol. 29, no. 5, pp. 1092–1100, Sept 2006.

[9] E. Medagoda and P. Gibbens, "Synthetic-Waypoint Guidance Algorithm for Following a Desired Flight Trajectory," *AIAA Journal of Guidance, Control, and Dynamics*, vol. 33, no. 2, pp. 601–606, March 2010.

[10] N. Dhananjay and R. Kristiansen, "Guidance Strategy for Gradient Search by Multiple UAVs," in *AIAA Guidance, Navigation and Control Conference*, Dec 2012, AIAA 2012-4766, pp. 627–634.

[11] C.-K. Ryoo, H. Cho, and M.-J. Tahk, "Optimal guidance laws with terminal impact angle constraint," *Journal of Guidance, Control, and Dynamics*, vol. 28, no. 4, pp. 724–732, 2005.

[12] A. Ratnoo, S. Hayoun, A. Granot, and T. Shima, "Path Following Using Trajectory Shaping Guidance," *AIAA Journal of Guidance, Control, and Dynamics*, vol. 38, no. 1, pp. 106–116, Jan 2015.

[13] N. Shneydor, *Missile Guidance and Pursuit - Kinematics, Dynamics and Control*. Chichester: Harwood Publishing, 1998.

[14] P. Zarchan, *Tactical and strategic missile guidance*. Washington, DC: In Progress in Astronautics and Aeronautics, Vol. 124, 1990.

[15] M. Guelman, "A qualitative study of proportional navigation," *IEEE Transactions on Aerospace and Electronic Systems*, vol. 4, no. AES-7, pp. 637–643, 1971.

[16] ——, "Proportional navigation with a maneuvering target," *IEEE Transactions on Aerospace and Electronic Systems*, vol. 3, no. AES-8, pp. 364–371, 1972.

[17] K. Becker, "Closed-form solution of pure proportional navigation," *Aerospace and Electronic Systems, IEEE Transactions on*, vol. 26, no. 3, pp. 526–533, 1990.

[18] D. Ghose, "True proportional navigation with maneuvering target," *Aerospace and Electronic Systems, IEEE Transactions on*, vol. 30, no. 1, pp. 229–237, 1994.

[19] V. Garber, "Optimum intercept laws for accelerating targets." *AIAA Journal*, vol. 6, no. 11, pp. 2196–2198, 1968.

[20] K. Babu, I. Sarma, and K. Swamy, "Switched bias proportional navigation for homing guidance against highly maneuvering targets," *Journal of Guidance, Control, and Dynamics*, vol. 17, no. 6, pp. 1357–1363, 1994.

[21] O. Ariff, R. Zbikowski, A. Tsourdos, and B. White, "Differential geometric guidance based on the involute of the target's trajectory," *Journal of guidance, control, and dynamics*, vol. 28, no. 5, pp. 990–996, 2005.

[22] A. E. Bryson and Y. C. Ho, *Applied Optimal Control Optimization, Estimation and Control*. New York: Taylor and Francis, 1975.

[23] M. A. Day, M. R. Clement, J. D. Russo, D. Davis, and T. H. Chung, "Multi-UAV Software Systems and Simulation Architecture," in *2015 International Conference on Unmanned Aerial Systems*. Denver, CO: IEEE, 2015, pp. 426–435.

[24] T. H. Chung, M. R. Clement, M. A. Day, K. Jones, D. Davis, and M. Jones, "Live-Fly, Large-Scale Field Experimentation for Large Numbers of Fixed-Wing UAVs," in *2016 IEEE International Conference on Robotics and Automation*, Stockholm, Sweden, 2016.

[25] A. Ratnoo and D. Ghose, "Impact angle constrained interception of stationary targets," *Journal of Guidance, Control, and Dynamics*, vol. 31, no. 6, pp. 1817–1822, 2008.

[26] B. Kim, J. Lee, and H. Han, "biased png law for impact with angular constraint," *Aerospace and Electronic Systems, IEEE Transactions on*, vol. 34, no. 1, pp. 277–288, 1998.

[27] S. Ghosh, D. Ghose, and S. Raha, "Composite Guidance for Impact Angle Control Against Higher Speed Targets," *Journal of Guidance, Control, and Dynamics*, vol. 39, no. 1, pp. 98–117, 2016.

[28] S. Ghosh, O. Yakimenko, D. Davis, and T. Chung, "Unmanned Aerial Vehicle Guidance for an All-Aspect Approach to a Stationary Point," Accepted for *Journal of Guidance, Control, and Dynamics*.

[29] S. Ghosh, D. Ghose, and S. Raha, "Unified Time-to-go Algorithms for Proportional Navigation Class of Guidance," *Journal of Guidance, Control, and Dynamics*, vol. 39, no. 6, pp. 1188–1205, 2016.